HYDROLOGICAL PROCESSES
Hydrol. Process. **24**, 1343–1356 (2010)
Published online 17 February 2010 in Wiley InterScience
(www.interscience.wiley.com) DOI: 10.1002/hyp.7597

Isotopic composition ($\delta^{18}O$ and δD) of precipitation and groundwater in a semi-arid, mountainous area (Guadiana Menor basin, Southeast Spain)

F. Fernández-Chacón,[1]* J. Benavente,[1] J. C. Rubio-Campos,[2] C. Kohfahl,[3] J. Jiménez,[1] H. Meyer,[4] H. Hubberten[4] and A. Pekdeger[3]

[1] *Instituto del Agua, Universidad de Granada, Water Research Institute, c/Ramón y Cajal 4, 18071 Granada, Spain*
[2] *Instituto Geológico y Minero de España, Oficina de Proyectos de Granada, Urbanización Alcázar del Genil 4, Edificio Zulema bajo, 18006 Granada, Spain*
[3] *Freie Universität Berlin, Institute of Geological Sciences, Malteserstr 74-100, D-12249 Berlin, Germany*
[4] *Alfred Wegener Institute, Telegrafenberg A43, D-1°4473 Potsdam, Germany*

Abstract:

We characterize the precipitation and groundwater in a mountainous (peaks slightly above 3000 m a.s.l.), semi-arid river basin in SE Spain in terms of the isotopes ^{18}O and ^{2}H. This basin, with an extension of about 7000 km^2, is an ideal site for such a study because fronts from the Atlantic and the Mediterranean converge here. Much of the land is farmed and irrigated both by groundwater and runoff water collected in reservoirs. A total of approximately 100 water samples from precipitation and 300 from groundwater have been analysed. To sample precipitation we set up a network of 39 stations at different altitudes (800–1700 m a.s.l.), with which we were able to collect the rain and snowfall from 29 separate events between July 2005 and April 2007 and take monthly samples during the periods of maximum recharge of the aquifers. To characterize the groundwater we set up a control network of 43 points (23 springs and 20 wells) to sample every 3 months the main aquifers and both the thermal and non-thermal groundwater. We also sampled two shallow-water sites (a reservoir and a river). The isotope composition of the precipitation forms a local meteoric water line (LMWL) characterized by the equation $\delta D = 7{\cdot}72\delta^{18}O + 9{\cdot}90$, with mean values for $\delta^{18}O$ and δD of $-10{\cdot}28‰$ and $-69{\cdot}33‰$, respectively, and $12{\cdot}9‰$ for the d-excess value. To correlate the isotope composition of the rainfall water with groundwater we calculated the weighted local meteoric water line (WLMWL), characterized by the equation $\delta D = 7{\cdot}40\delta^{18}O + 7{\cdot}24$, which takes into account the quantity of water precipitated during each event. These values of $(d\delta D/d\delta^{18}O)<8$ and d-excess $(\delta D - 8\delta^{18}O)<10$ in each curve bear witness to the 'amount effect', an effect which is more manifest between May and September, when the ground temperature is higher. Other effects noted in the basin were those of altitude and the continental influence. The isotopic compositions of the groundwater are represented by the equation $\delta D = 4{\cdot}79\delta^{18}O - 18{\cdot}64$. The groundwater is richer in heavy isotopes than the rainfall, with mean values of $-8{\cdot}48‰$ for $\delta^{18}O$ and $-59{\cdot}27‰$ for δD. The isotope enrichment processes detected include a higher rate of evaporation from detrital aquifers than from carbonate ones, the effects of recharging aquifers from irrigation return flow and/or from reservoirs' leakage and enrichment in $\delta^{18}O$ from thermal water. Copyright © 2010 John Wiley & Sons, Ltd.

KEY WORDS stable isotopes; precipitation; local meteoric water line; groundwater; southeast Spain

Received 27 June 2009; Accepted 30 November 2009

INTRODUCTION

Since the 1960s an understanding of the isotope composition of water has become an essential element in characterizing hydrogeological processes, and the isotope composition of atmospheric precipitation has become a key tool for hydrogeologists, meteorologists and climatologists alike. The isotopes most commonly referred to are those of the water molecule itself, ^{18}O and ^{2}H, because of their value in tracing water and the processes that affect it (Gat and Matsui, 1991). The relationship between the isotopes of water and d-excess ($\delta D - 8\delta^{18}O$) can be used to explore the origins of precipitation, the fronts that contribute to recharging the aquifers in the basin in question, the rates of recharge and the processes influencing final isotope composition. The d-excess value is arrived at during evaporation of the water producing the vapour in the clouds and does not vary significantly during the later development of the cloud mass; it thus constitutes a highly valuable indicator of the area where the water vapour was produced (Rindsberger *et al.*, 1983; Cruz-San Julián *et al.*, 1992; Celle-Jeanton *et al.*, 2001). High d-excess values are associated with a deficit in humidity over the ocean, whereas low values point to high atmospheric humidity (Clark and Fritz, 1997). Values of around 10‰ indicate waters of Atlantic origin, whilst values closer to 20‰ indicate waters from the eastern Mediterranean (Gat and Carmi, 1970; Celle-Jeanton *et al.*, 2001; IAEA, 2001; Vandenschrick *et al.*, 2002; Bowen and Revenaugh, 2003; Aouad *et al.*, 2004), although some authors have proposed higher values (up

* Correspondence to: F. Fernández-Chacón, Instituto del Agua, Universidad de Granada, Water Research Institute, c/Ramón y Cajal 4, 18071 Granada, Spain. E-mail: paquifchacon@gmail.com

to 32‰: Gat and Carmi, 1970; Gat and Dansgaard, 1972; Rindsberger *et al*., 1983; Gat and Carmi, 1987). On the other hand, values close to 14‰ would indicate waters proceeding from the western Mediterranean (Gat and Carmi, 1970; Celle-Jeanton *et al*., 2001; Vandenschrick *et al*., 2002; Andreo *et al*., 2004).

The southeastern Iberian Peninsula is a particularly interesting area for the development of research into environmental isotopes in precipitation. Situated between the Mediterranean Sea and the Atlantic Ocean, it presents a complex orography including the Betic Cordilleras. This southwest–northeast trending Alpine mountainous belt features striking variations in altitude in a matter of some few kilometres. Although the climate is predominantly Mediterranean, the spatial distribution of the mountain chains gives rise to numerous zones of diverse local climates. Despite the obvious appeal of this context for research into isotopes, however, very few such studies have been carried out in the region (cf. Cruz-San Julián *et al*., 1992; Andreo *et al*., 2004; Kohfahl *et al*., 2008a).

The first precipitation samples taken in the Iberian Peninsula for the purpose of isotope analysis were obtained by the IAEA in 1962 through its global monitoring network, the International Atomic Energy Agency and World Meteorological Organization (IAEA-WMO). With the incorporation of the Gibraltar station into its control network this was subsequently expanded after 1978.

Early research into the isotope content of precipitation in southeastern Spain was carried out by Cruz-San Julián *et al*. (1992), who focused on a northwest–southeast Cazorla range–Mediterranean coast transverse profile. Integration of their data revealed that the aquifers were recharged mainly during the winter months with precipitation proceeding mostly from Atlantic fronts, and that in the study zone evaporation could occur before precipitation was infiltrated in the soil.

After 2 years, Plata (1994) led a study of the isotope composition of precipitation and groundwater spanning the entire Iberian Peninsula. All these data were used to produce the first meteoric water line of the Iberian Peninsula at a regional level: $\delta D = (7{\cdot}79 \pm 0{\cdot}62)\ \delta^{18}O + (10{\cdot}02 \pm 2{\cdot}75)$. This study also reported the partial evaporation of cloud water as well as evaporation during its fall to the earth throughout the peninsula. The author drew up the first map showing the distribution of $\delta^{18}O$ in groundwater, highlighting the great influence of orographic systems on the distribution of isotope values, and defined the main entry points of cloud fronts into the peninsula: to the west (from fronts generated in the Atlantic to the northwest of the peninsula over Galicia and to the southwest by way of the Gulf of Cádiz) and to the east and northeast from fronts generated in the Mediterranean (Plata, 1994).

The main aim of this study was to use isotopic tools to characterize the recharge patterns of the semi-arid Guadiana Menor basin. We investigated the isotope content of the precipitation and determined the local meteoric water line (LMWL) and weighted local meteoric water line (WLMWL). We then compared the LMWL with the local groundwater line (LGWL) to determine recharge due to precipitation and the effects of reservoirs and irrigation on this particular hydrological system. Provided the above-mentioned variety of topographic and climatic conditions in a relatively small study area, which allows a favourable framework for the interpretation of environmental stable isotope data, this research leads to improve the current understanding of recharge processes in intramontane basins under semi-arid conditions.

STUDY AREA

The river Guadiana Menor basin is the easternmost subbasin of the river Guadalquivir, in southern Spain and covers a surface area of 7192 km^2. It is bordered by high mountainous relief with maximum altitudes of 2270 m a.s.l. in the Sierra de Baza range and 3138 m a.s.l. in the Sierra Nevada range to the south; 2167 m a.s.l. in the mountain ranges to the west; 2382 m a.s.l. in the Cazorla-Segura ranges to the north and 2045 m a.s.l. in the easternmost reliefs (Figure 1).

The Guadiana Menor basin has a semi-arid climate. Its intensive agricultural activity is subject to considerable drought stress because of a recent increase in the number and length of periods without rain. Lying between 80 and 200 km from the Mediterranean coast it harbours a great variety of aquifers, from the geological and hydrogeological standpoint, and groundwaters of widely varying temperatures (from 10 to 45 °C), which have hardly been studied to date.

In southern and southeastern Spain precipitation derives from both the Atlantic and Mediterranean, although in the Guadiana Menor basin the abrupt features of the relief and the great altitude of the ranges to the northwest (Cazorla and Segura) and southwest (Sierra Nevada) limit the influence of the Atlantic fronts (Cruz-San Julián *et al*., 1992; Plata, 1994). In a study of the southeast of the Peninsula, Plata (1994) suggested that Atlantic fronts represented 66–69% of the total volume of precipitation and that Mediterranean fronts accounted for 11–21%.

According to data from the Junta de Andalucía weather stations, the average rainfall in the study area is around 350 mm/year and occurs mainly in the winter (Figure 1). The aquifers found in the mountainous sectors are made up of limestones, dolomites and calcarenites; in the lower, central parts of the basin the aquifers are made up of detrital materials (conglomerates, gravels, sands and silts) with which a hydraulic connection normally exists (Figure 1). Intensive agricultural activity takes place in the basin, particularly over recent years, for the most part upon detrital materials surrounding the carbonate outcrops.

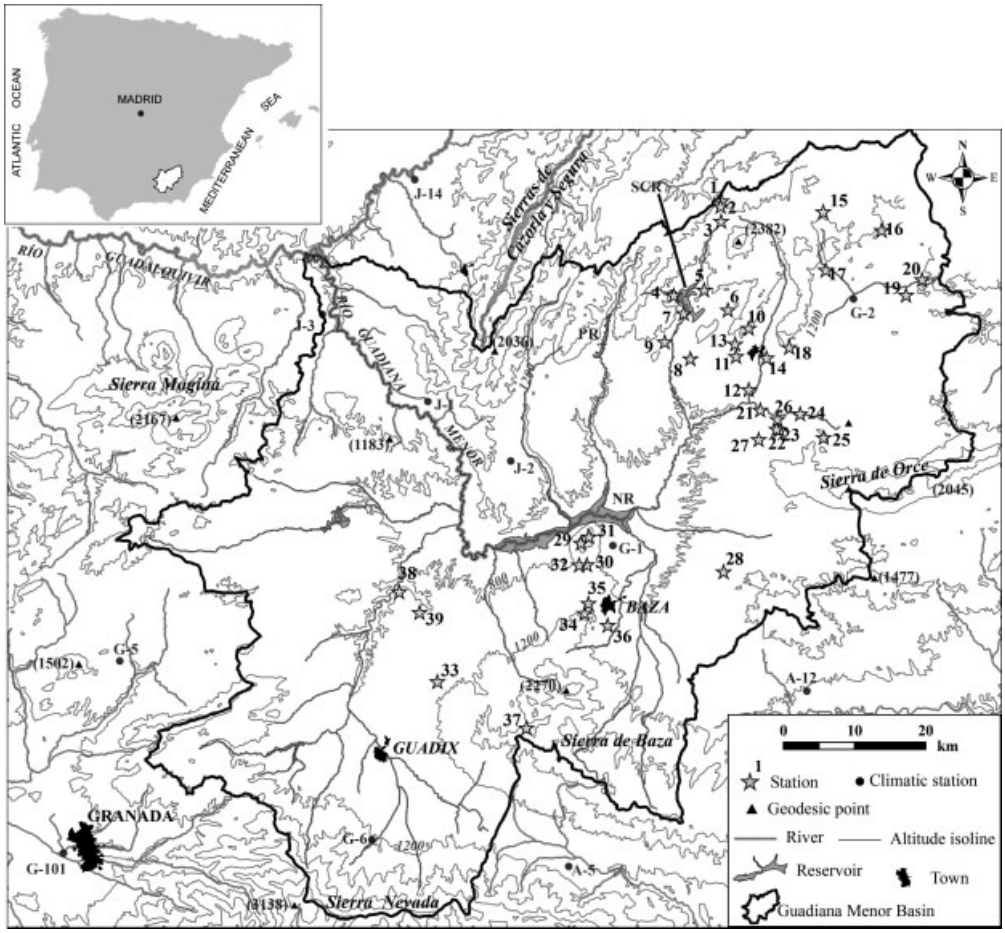

Figure 1. Location and topography of the Guadiana Menor basin. Star symbols indicate the precipitation sampling stations used. NR: Negratín reservoir; PR: Portillo reservoir; SCR: San Clemente reservoir

METHODS

From September 2005 to April 2007 a total of 98 precipitation samples were obtained in the central, eastern and northeastern zones of the Guadiana Menor basin from 39 stations (Table I), of which 27 were situated in the northeastern section and 12 in the central area of the basin, in order to carry out a representative sampling of each slope at different altitudes (Figure 1). Over that period, 29 individual precipitation events were sampled at 2–19 different stations (Table II). Furthermore, monthly rainfall in May 2006 and April 2007 was analysed at 10 and 19 stations, respectively. These were the months with highest precipitation during the sampling period. The maximum number of events (27) was sampled in station 37. The criteria used for the selection of the sampling network of individual and monthly events were (i) even spatial distribution, (ii) different altitudes and (iii) easy access.

The technical procedure carried out for sampling the precipitation waters for isotope analysis was as follows. A 1-l polyethylene bottle with a funnel covered with mesh to impede the entry of external elements was used to monitor short-duration storm events. These bottles were gathered just a few hours after the storm so that the isotope contents would not be altered by evaporation processes within the recipient. For cumulative precipitation episodes over a 1-month period, a 5-l polyethylene bottle with a mesh-protected funnel, containing paraffin oil to impede evaporation was used (OIEA, 1996). The recipients were installed at different altitudes on various slopes in secluded areas free of trees and large shrubs and were held in place using stones to prevent them from tipping over.

Between July 2005 and April 2007, 45 groundwater points were sampled: 23 springs, 20 wells (in operation) and 2 shallow waters (Table III and Figure 2). The groundwater sampling involved significant springs and wells with known lithological columns and drilled depths, distributed over different aquifers throughout the eastern, northeastern and central areas of the Guadiana Menor river basin, from the recharge zones (carbonate aquifers) to the discharge zones (detrital aquifers). Each point was sampled every 3 months along the study period. The variation coefficients obtained, between 0·1% and 3%, indicate fairly uniform values. In the Table III the average isotopic contents for each point are presented.

All the water samples were put into hermetic 50 ml polyethylene flasks and kept cold until being subject to isotope analysis at the Alfred Wegener Institut (AWI) in Potsdam (Germany), using Finnigan Mat Delta-S mass spectrometers and the equilibrium method (Meyer *et al.*, 2000). Measurement precision is approximately 0·1‰

Table I. Main characteristics of the precipitation sampling stations in the study area (see also Figure 1). Maximum, minimum and mean values (weighted as a function of the quantity of precipitation) of the isotope composition of precipitation are indicated

Number of station	Site	X (UTM)	Y (UTM)	Altitude (m)	N° Analyses	Amount of precipitation (mm)	^{18}O Max	D Max	^{18}O Min	D Min	Weighted ^{18}O	Weighted D	Weighted d-excess
1	Cañalonguillo	535 932	4 206 383	1760	4	27	−2·89	−16·10	−10·74	−75·36	−10·58	−74·18	10·48
2	Puerto de la Losa	535 814	4 205 597	1685	2	173	−3·38	−18·33	−9·00	−57·89	−5·48	−33·09	10·73
3	Cruce Puerto-PDF	535 850	4 203 491	1330	2	75	−9·83	−67·18	−13·87	−103·88	−10·38	−72·17	10·87
5	Casa en Ruinas	533 459	4 193 825	1140	2	94	−9·30	−62·17	−16·03	−112·01	−13·90	−96·24	14·96
6	Mazagrande	536 814	4 190 993	1080	1	7	−7·05	−45·67	−7·05	−45·67	−7·05	−45·67	10·70
7	Aparcamiento	530 598	4 190 520	1074	1	30	−15·41	−106·40	−15·41	−106·40	−15·41	−106·40	16·87
8	Canteras	531 521	4 184 131	1020	2	40	−12·68	−92·48	−15·32	−108·49	−14·65	−104·42	13·15
9	Carretera Duda	527 942	4 186 508	1030	1	30	−14·44	−99·99	−14·44	−99·99	−14·44	−99·99	15·53
10	Cerro Perico Ruíz	539 733	4 188 451	1404	4	189	−4·28	−23·68	−13·34	−97·53	−11·56	−81·41	11·04
11	Parpacén	537 979	4 184 452	922	2	40	−12·75	−92·98	−13·64	−94·81	−13·42	−93·45	13·89
12	Ctjo. los Nogales	539 750	4 179 775	855	3	38	−2·94	−12·56	−7·01	−46·10	−3·07	−13·66	10·94
13	Desvío Puerto	537 850	4 186 200	1000	2	94	−9·62	−65·56	−15·16	−105·14	−13·41	−92·62	14·68
14	Fuencaliente	542 250	4 184 250	912	1	30	−14·35	−93·15	−14·35	−93·15	−14·35	−93·15	21·68
15	Cortijo Moya	550 231	4 204 850	1267	2	173	−4·39	−24·34	−9·17	−62·15	−6·17	−38·45	10·94
16	Cortijo Porche	558 450	4 202 240	1160	1	10	−12·72	−95·95	−12·72	−95·95	−12·72	−95·95	5·77
17	Pedania Lóbrega	550 568	4 196 635	1076	3	101	−6·60	−44·68	−13·88	−89·07	−12·18	−79·52	17·92
18	Cortijo San Juan	545 443	4 185 741	1070	5	219	−4·17	−23·56	−14·24	−102·08	−11·19	−74·05	15·40
19	Bugéjar	561 863	4 193 083	1050	2	75	−9·59	−64·14	−13·64	−99·79	−10·14	−68·99	12·00
20	Collado Cobatillas	564 155	4 195 282	1151	1	64	−9·37	−62·71	−9·37	−62·71	−9·37	−62·71	12·25
21	Río Orce	541 380	4 176 927	840	1	30	−15·22	−105·64	−15·22	−105·64	−15·22	−105·64	16·11
22	Cerro Taales	544 086	4 174 133	1070	2	75	−7·66	−52·73	−11·65	−80·12	−8·20	−56·46	9·17
23	Llano Taales	543 678	4 174 222	990	2	40	−11·70	−86·52	−14·14	−92·34	−13·52	−90·87	17·29
24	Cementerio	546 983	4 176 377	960	2	173	−4·16	−22·43	−7·99	−53·60	−5·59	−34·06	10·63
25	Sierra Umbría	550 276	4 173 044	1290	2	173	−4·58	−22·85	−7·98	−49·65	−5·85	−32·85	13·97
26	Fuencaliente Orce	543 780	4 175 600	885	1	30	−14·32	−93·81	−14·32	−93·81	−14·32	−93·81	20·78
27	Cortijo Victor	541 150	4 172 750	945	1	30	−15·75	−109·80	−15·75	−109·80	−15·75	−109·80	16·19
28	Don Ramón	536 200	4 154 100	995	1	41	−14·51	−97·33	−14·51	−97·33	−14·51	−97·33	18·77
29	Pico del Jabalcón	516 149	4 158 153	1484	3	111	−4·30	−21·25	−12·20	−85·55	−7·31	−45·07	13·42
30	Llanos de Catín	516 968	4 155 096	993	2	101	−3·10	−14·83	−8·24	−52·78	−5·96	−35·94	11·73
31	Curva Jabalcón	517 295	4 159 059	1160	1	56	−6·03	−40·82	−6·03	−40·82	−6·03	−40·82	7·41
32	Fuente Grande	515 898	4 155 072	877	1	51	−15·00	−102·06	−15·00	−102·06	−15·00	−102·06	17·96
33	Cortijo Conejo	495 990	4 138 650	1130	1	41	−15·06	−102·14	−15·06	−102·14	−15·06	−102·14	18·32
34	La Atalaya	516 665	4 148 257	1110	2	55	−3·70	−16·72	−11·86	−81·04	−5·20	−28·59	13·03
35	Llanos de Cuquillo	517 200	4 149 650	1025	2	97	−7·69	−53·58	−15·11	−103·02	−11·99	−82·22	13·70
36	Siete Fuentes	519 920	4 146 552	905	1	10	−12·13	−87·06	−12·13	−87·06	−12·13	−87·06	9·98
37	Las Juntas	508 500	4 132 120	1100	27	202	−2·35	−1·09	−16·52	−123·46	−7·69	−48·17	13·39
38	Cerro la Raja	490 606	4 151 266	815	2	101	−5·66	−37·23	−8·83	−57·98	−7·43	−48·78	10·65
39	Mirador Gorafe	493 475	4 148 375	990	1	56	−8·66	−56·36	−8·66	−56·36	−8·66	−56·36	12·94
Mean						78							
Max							−2·35	−1·09					
Min									−16·52	−123·46			
Mean											−10·66	−71·69	13·56

Table II. Isotope analysis of precipitation from 2005 to 2007 in chronological order of the events

Number of station	Sampling date	Altitude (m a.s.l.)	Amount of precipitation (mm)	$\delta^{18}O$ (‰)	δD (‰)	d-excess (‰)
1	24 Jul-2005	1760	0·10	−3·97	−23·40	8·34
1	10 Aug-2005	1760	0·39	−2·89	−16·10	7·01
1	8 Sep-2005	1760	26·80	−10·74	−75·36	10·54
12	13/17 Sep-2005	855	1·20	−7·01	−46·10	10·02
37	13/17 Sep-2005	1100	17·20	−6·80	−42·47	11·91
6	13/17 Sep-2005	1080	6·73	−7·05	−45·67	10·70
10	13/17 Sep-2005	1404	6·73	−8·05	−48·89	15·53
17	13/17 Sep-2005	1076	6·73	−6·60	−44·68	8·12
18	13/17 Sep-2005	1070	6·73	−7·39	−47·61	11·53
1	04 Oct-2005	1760	0·10	−5·85	−35·68	11·13
37	12 Oct-2005	1100	3·00	−9·48	−61·61	14·19
37	11 Nov-2005	1100	0·40	−8·12	−43·53	21·43
37	21 Nov-2005	1100	8·60	−7·03	−38·75	17·49
10	29/31 Jan-2006	1404	10·14	−13·34	−97·53	9·19
3	29/31 Jan-2006	1330	10·14	−13·87	−103·88	7·08
4	29/31 Jan-2006	1120	10·14	−13·46		
8	29/31 Jan-2006	1020	10·14	−12·68	−92·48	8·92
11	29/31 Jan-2006	922	10·14	−12·75	−94·81	7·19
16	29/31 Jan-2006	1160	10·14	−12·72	−95·95	5·77
18	29/31 Jan-2006	1070	10·14	−13·76	−102·08	8·00
19	29/31 Jan-2006	1050	10·14	−13·64	−99·79	9·33
22	29/31 Jan-2006	1070	10·14	−11·65	−80·12	13·08
23	29/31 Jan-2006	990	10·14	−11·70	−86·52	7·08
29	29/31 Jan-2006	1484	10·14	−12·20	−85·55	12·05
32	29/31 Jan-2006	877	10·14	−10·87		
34	29/31 Jan-2006	1110	10·14	−11·86	−81·04	13·81
36	29/31 Jan-2006	905	10·14	−12·13	−87·06	9·98
37	09 Feb-2006	1100	0·20	−13·86	−107·01	3·88
37	19 Feb-2006	1100	10·40	−10·12	−69·15	11·81
37	05 Mar-2006	1100	11·00	−12·06	−89·63	6·85
37	11 Mar-2006	1100	0·10	−11·58	−79·93	12·71
37	18/20 Mar-2006	1100	2·60	−7·32	−52·67	5·87
37	18/20 Mar-2006	1100	2·20	−9·18	−63·70	9·78
37	15 Apr-2006	1100	5·40	−2·35	−1·09	17·70
37	22 Apr-2006	1100	29·80	−6·13	−34·26	14·77
37	23 Apr-2006	1100	1·20	−9·82	−66·01	12·58
37	28 Apr-2006	1100	4·00	−4·73	−26·37	11·45
37	03/05 May-2006	1100	7·80	−4·44	−20·98	14·52
12	03/05 May-2006	855	34·00	−2·94	−12·56	10·96
12	03/05 May-2006	855	2·60	−3·03	−13·16	11·08
37	03/05 May-2006	1100	0·60	−4·62	−21·82	15·15
37	11 May-2006	1100	0·20	0·52	5·17	0·99
37	30/31 May-2006	1100	0·20	−5·96	−35·91	11·81
37	30/31 May-2006	1100	29·20	−4·94	−26·47	13·05
2	All May-2006	1685	108·20	−3·38	−18·33	8·71
10	All May-2006	1404	108·20	−4·28	−23·68	10·56
15	All May-2006	1267	108·20	−4·39	−24·34	10·78
18	All May-2006	1070	108·20	−4·17	−23·56	9·80
24	All May-2006	960	108·20	−4·16	−22·43	10·83
25	All May-2006	1290	108·20	−4·58	−22·85	13·82
29	All May-2006	1484	44·80	−4·30	−21·25	13·14
30	All May-2006	993	44·80	−3·10	−14·83	9·98
34	All May-2006	1110	44·80	−3·70	−16·72	12·85
38	All May-2006	815	44·80	−5·66	−37·23	8·09
37	01 Sep-2006	1100	0·20	−5·95	−40·75	6·83
14	26/29 Jan-2007	912	29·80	−14·35	−93·15	21·68
17	26/29 Jan-2007	1076	29·80	−13·88	−89·07	21·95
18	26/29 Jan-2007	1070	29·80	−14·24	−92·33	21·57
23	26/29 Jan-2007	990	29·80	−14·14	−92·34	20·76
26	26/29 Jan-2007	885	29·80	−14·32	−93·81	20·78
28	26/29 Jan-2007	995	40·80	−14·51	−97·33	18·77
32	26/29 Jan-2007	877	40·80	−15·00	−102·06	17·96
33	26/29 Jan-2007	1130	40·80	−15·06	−102·14	18·32
35	26/29 Jan-2007	1025	40·80	−15·11	−103·02	17·86

Table II. (*Continued*)

Number of station	Sampling date	Altitude (m a.s.l.)	Amount of precipitation (mm)	$\delta^{18}O$ (‰)	δD (‰)	d-excess (‰)
37	26/29 Jan-2007	1100	40·80	−12·12	−79·77	17·18
5	26/29 Jan-2007	1140	29·80	−16·03	−112·01	16·20
7	26/29 Jan-2007	1074	29·80	−15·41	−106·40	16·87
8	26/29 Jan-2007	1020	29·80	−15·32	−108·49	14·58
9	26/29 Jan-2007	1030	29·80	−14·44	−99·99	15·53
11	26/29 Jan-2007	922	29·80	−13·64	−92·98	16·17
13	26/29 Jan-2007	1000	29·80	−15·16	−105·14	16·17
21	26/29 Jan-2007	840	29·80	−15·22	−105·64	16·11
27	26/29 Jan-2007	945	29·80	−15·75	−109·80	16·19
37	20 Feb-2007	1100	3·00	−16·52	−123·46	8·72
37	01 Mar-2007	1100	0·20	−13·61	−98·39	10·49
37	26 Mar-2007	1100	5·80	−7·71	−48·21	13·50
37	29 Mar-2007	1100	0·40	−16·02	−113·77	14·37
37	04 Apr-2007	1100	4·60	−10·17	−62·67	18·71
37	11 Apr-2007	1100	3·20	−4·07	−12·55	19·97
2	all Apr-2007	1685	64·40	−9·00	−57·89	14·14
3	all Apr-2007	1330	64·40	−9·83	−67·18	11·46
5	all Apr-2007	1140	64·40	−9·30	−62·17	12·27
10	all Apr-2007	1404	64·40	−10·07	−66·83	13·77
13	all Apr-2007	1000	64·40	−9·62	−65·56	11·44
15	all Apr-2007	1267	64·40	−9·17	−62·15	11·20
17	all Apr-2007	1076	64·40	−9·77	−66·77	11·41
18	all Apr-2007	1070	64·40	−9·30	−65·07	9·21
19	all Apr-2007	1050	64·40	−9·59	−64·14	12·42
20	all Apr-2007	1151	64·40	−9·37	−62·71	12·25
22	all Apr-2007	1070	64·40	−7·66	−52·73	8·56
24	all Apr-2007	960	64·40	−7·99	−53·60	10·30
25	all Apr-2007	1290	64·40	−7·98	−49·65	14·22
29	all Apr-2007	1484	56·20	−8·83	−56·76	13·88
30	all Apr-2007	993	56·20	−8·24	−52·78	13·13
31	all Apr-2007	1160	56·20	−6·03	−40·82	7·41
35	all Apr-2007	1025	56·20	−7·69	−53·58	7·96
38	all Apr-2007	815	56·20	−8·83	−57·98	12·69
39	all Apr-2007	990	56·20	−8·66	−56·36	12·94

for $\delta^{18}O$ and 0·8‰ for δD. AWI laboratory standards were used, calibrated with reference to the Vienna standard mean ocean water (V-SMOW). The results of isotope composition are expressed as per mille deviations from the internationally accepted V-SMOW standard (Gonfiantini, 1978). Analytical error is ±0·07‰ for $\delta^{18}O$ and ±0·7‰ for δD. The mean weighted $\delta^{18}O$ and δD composition of rainfall at each rain gauge was determined by the following equation (Paternoster *et al.*, 2008):

$$R_{mw} = \Sigma^{n}{}_{i=1} P_i \ \delta X_i / \Sigma^{n}{}_{i=1} P_i$$

where P_i is the precipitation events, n is the number of events and δX_i refers to either $\delta^{18}O$ or δD composition of the precipitation events.

RESULTS AND DISCUSSION

Precipitation

In a situation of increased drought stress in south/southeast Spain, largely due to the expansion of agriculture and tourism, but aggravated by a general decline in precipitation, the first isotope studies to characterize the hydrogeology of local aquifers were recently carried out in the early years of this century (Vandenschrick *et al.*, 2002; Andreo *et al.*, 2004; Frot *et al.*, 2007). The LMWLs obtained to date in southeast Spain are $\delta D = 7{\cdot}13\delta^{18}O + 9{\cdot}75$ with $R^2 = 0{\cdot}95$ (Cruz-San Julián *et al.*, 1992) and $\delta D = 7{\cdot}00\delta^{18}O + 6{\cdot}05$ with $R^2 = 0{\cdot}88$ (Andreo *et al.*, 2004).

Over the study period, the evolution of precipitation in the basin is shown in the Figure 3. Agro-climatic stations at intermediate altitudes were used (Figure 1), and thus did not record precipitation at high altitudes (www.juntadeandalucia.es/...).

Stable isotopes and LMWL. Figure 4 and Table II illustrate the δ values, ranging from −2·35‰ to −16·52‰ for $\delta^{18}O$, with a weighted mean value of −10·28‰; from −1·1‰ to −123·5‰ for δD, with a mean of −69·3‰; and from 21·68‰ to 5·77‰ for *d*-excess, with a mean of 12·90‰ (Table I).

The corresponding equations of the meteoric water lines shown in Figure 4 are compiled in the following:

Equations obtained in this research

1. LMWL $\delta D = 7{\cdot}72\delta^{18}O + 9{\cdot}90$, with $R^2 = 0{\cdot}98$

Table III. Average isotope contents of groundwater and shallow water (values in ‰). S = springs, with indication of the average flow or flow range (Q). W = drilled wells in operation, with indication of the correspondent depth. R = shallow water. The type of aquifer related with each sampling point is also indicated

Reference	Aquifer	Q(l/s)	$\delta^{18}O$	δD	d-excess
S-1	Carbonatic	25	−9·01	−59·70	12·40
S-2	Carbonatic	20	−8·90	−59·25	11·98
S-3	Detrital	0·25	−8·04	−57·15	7·17
S-4	Carbonatic	25	−9·22	−61·56	12·20
S-5	Detrital	7	−8·48	−58·57	9·27
S-6	Detrital	0·5	−8·66	−59·65	9·63
S-7	Detrital	75	−8·09	−56·88	7·88
S-8	Detrital	15	−8·86	−62·15	8·70
S-9	Carbonatic	0.2	−8·02	−55·66	8·46
S-10	Detrital	3	−7·99	−54·90	8·98
S-11	Detrital	7	−8·53	−58·81	9·45
S-12	Detrital	25–140	−8·61	−58·65	10·20
S-13	Detrital	8–21	−7·73	−56·22	5·59
S-14	Detrital	200	−9·39	−62·62	12·47
S-15	Carbonatic	10	−8·97	−61·30	10·62
S-16	Carbonatic	1	−9·38	−63·94	11·07
S-17	Carbonatic	10	−9·42	−66·77	8·57
S-18	Carbonatic	2	−9·55	−65·20	11·21
S-19	Carbonatic	25	−8·51	−57·48	10·58
S-20	Detrital	25	−9·90	−68·03	11·14
S-21	Detrital	5	−7·20	−55·48	2·12
S-22	Detrital	0·1	−6·99	−54·83	1·07
S-23	Carbonatic	2	−8·17	−58·48	6·78

Reference	Aquifer	Depth (m)	$\delta^{18}O$	δD	d-excess
W-1	Carbonatic	>85	−8·04	−58·75	5·59
W-2	Carbonatic	100	−6·92	−52·48	2·92
W-3	Carbonatic	127	−7·67	−55·30	6·07
W-4	Carbonatic	120	−7·65	−53·55	7·65
W-5	Detrital	90	−6·40	−48·11	3·06
W-6	Detrital	125	−8·89	−60·85	10·30
W-7	Carbonatic	90	−8·58	−60·26	8·38
W-8	Carbonatic	250	−8·78	−59·90	10·34
W-9	Detrital	120	−8·67	−59·23	10·11
W-10	Detrital	23	−8·37	−57·45	9·53
W-11	Carbonatic	100	−8·90	−60·61	10·62
W-12	Detrital	90	−9·24	−62·88	11·06
W-13	Carbonatic	135	−8·95	−60·34	11·23
W-14	Carbonatic	225	−9·28	−62·50	11·70
W-15	Carbonatic	175	−7·99	−58·56	8·52
W-16	Detrital	120	−8·94	−61·31	10·25
W-17	Carbonatic	410	−9·69	−68·69	8·80
W-18	Detrital	60	−7·31	−56·39	2·06
W-19	Detrital	110	−8·38	−62·23	4·80
W-20	Detrital	100	−9·15	−61·69	11·54

Reference	Aquifer	Q(l/s)	$\delta^{18}O$	δD	d-excess
R-1	Carbonatic		−7·02	−50·31	5·86
R-2	Carbonatic	100	−9·14	−62·68	10·42

2. WLMWL $\delta D = 7{\cdot}40\delta^{18}O + 7{\cdot}24$, with $R^2 = 0{\cdot}99$
   Reference equations
3. GMWL $\delta D = 8\delta^{18}O + 10$
4. WMMWL $\delta D = 8\delta^{18}O + 13{\cdot}7$
5. EMMWL $\delta D = 8\delta^{18}O + 22$.

The LMWL was derived using 96 unweighted precipitation samples out of 98 (Table II) because two samples contained a mistake in the determination of δD. The WLMWL was determined using the average stable isotope composition at each sampling location weighted for rainfall quantity (Table I).

The $d\delta D/d\delta^{18}O$ curve for these two lines is shallower than that for the GMWL and WMMWL (Figure 4), due to the rainfall events that occurred in spring and summer. These events reflect evaporation processes mainly between the months of May and September (with a concomitant enrichment in stable heavy isotopes) due to the higher temperature and the incidence of the quantity of rainfall (the so-called amount effect), an effect which is more manifest at this time of the year than in winter (Gedzelman *et al*., 1987). This effect typically refers to rainfall produced in large convective systems in the tropics where gradual rainout of moist air masses uplifted vertically to higher altitudes commonly occurs. In the latitudes of this study that effect can also be identified. It is characterized by an enrichment in heavy isotopes brought about by the evaporation of rain drops between leaving the cloud and reaching the earth, and/or an exchange of isotopes between the raindrops and atmospheric vapour (Dansgaard, 1953, 1961; Friedman *et al*., 1962; Ehhalt *et al*., 1963; Gedzelman *et al*., 1987), reaching at times positive values of $\delta^{18}O$ (Delgado *et al*., 1991, have observed this in the nearby Granada sector). The fact that the curve of the mean weighted values has a shallower slope than that of the LMWL indicates the amount effect.

Most of the points are situated between the GMWL and WMMWL, whilst just five samples (corresponding to the months of May, July, August and September) plot below the GMWL (Table II and Figure 5). Heavy-isotope enrichment processes during the summer months make it difficult to determine the origin of the weather fronts; *d*-excess depends upon changes in both $\delta^{18}O$ and δD, and during these months analytical uncertainty in this parameter can be quite high compared to its natural variability.

The samples collected in winter, on the other hand, are more depleted in heavy isotopes. Low surface temperatures inhibit isotope enrichment by the amount effect during these months. The snow samples from 2007 show the most negative values, plotting between the WMMWL and the EMMWL. In contrast, the rain samples corresponding to 28–31 January 2006 are aligned along the GMWL, indicating an Atlantic origin, which concurs with a low-pressure area over the Gulf of Cadiz (www.inm.es/es/eltiempo/observacion/satelite/masas). It is noteworthy that precipitation in the form of snow is produced by an additional kinetic isotopic fractioning, which may increase the *d*-excess in the water of the snowflake (Jouzel and Merlivat, 1984).

Precipitation in another meteorological events plots between the GMWL and the WMMWL, reflecting Atlantic and western Mediterranean origins, with a predominance of the former (Table II and Figure 5). On the

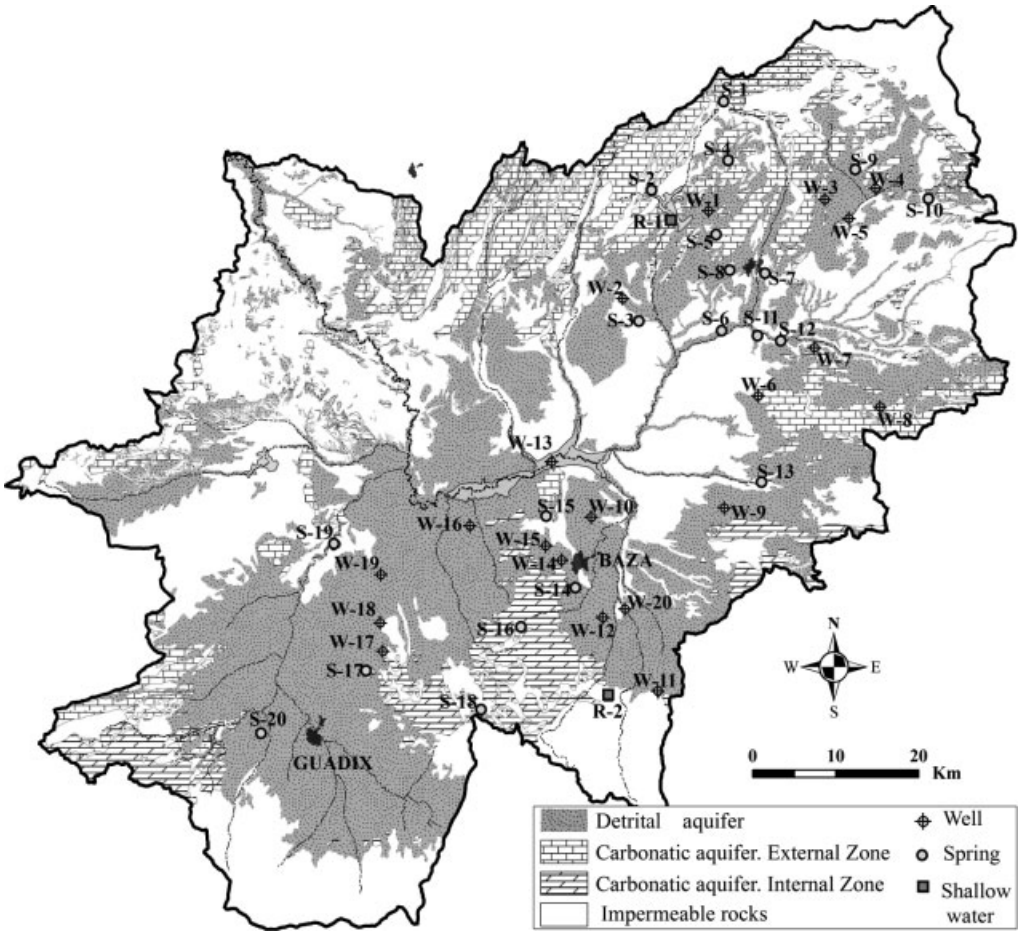

Figure 2. Map of the Guadiana Menor basin, showing the main aquifers and the groundwater and shallow-water points sampled

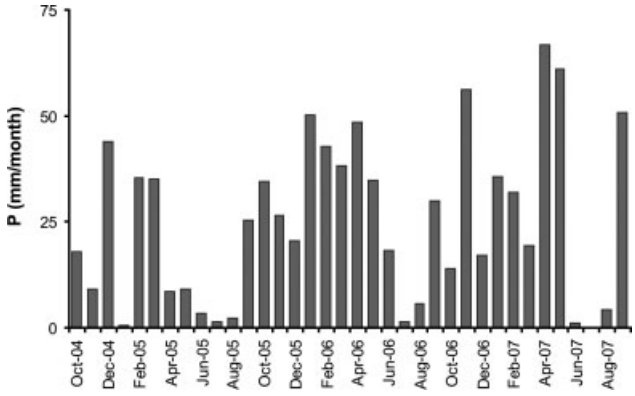

Figure 3. Evolution of average precipitation in the Guadiana Menor basin from 2001 to 2006 (hydrological year) (www.inm.es/es/eltiempo/observacion/satelite/masas)

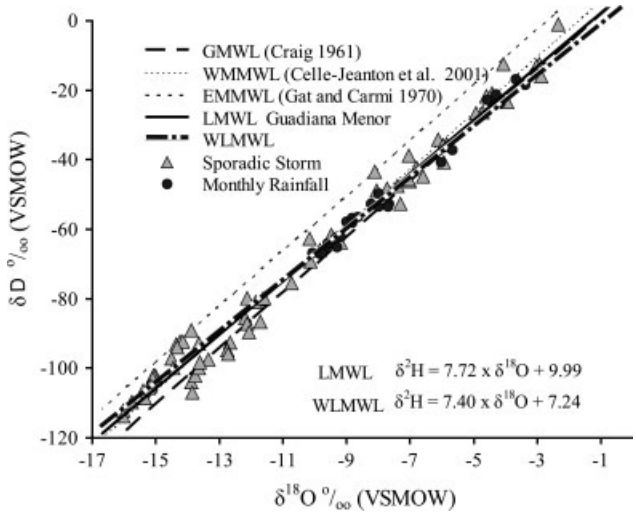

Figure 4. Plot of D versus ^{18}O contents of the precipitation samples collected in the Guadiana Menor basin from July 2005 to April 2007. Global meteoric water line (GMWL), western Mediterranean meteoric water line (WMMWL), eastern Mediterranean meteoric water line (EMMWL), local meteoric water line (LMWL) and weighted local meteoric water line (WLMWL) are shown

other hand, the individual rainfall event of November 2005 seems to be eastern Mediterranean in origin (Table II and Figure 5). The general influence of the Atlantic and the western Mediterranean is corroborated by the *d*-excess value, which is between the 10 of the GMWL (Craig, 1961a,b) and the 13·7 of the WMMWL (Celle-Jeanton *et al*., 2001).

The curve concurs with other LMWLs found by authors in the western (Iberian Peninsula) and central sectors of the Mediterranean (Italy and Tunisia) (see Table IV). Particularly, our LMWL is similar to those obtained previously in the regional context (Cruz-San Julián *et al*., 1992; Plata, 1994; Andreo *et al*., 2004).

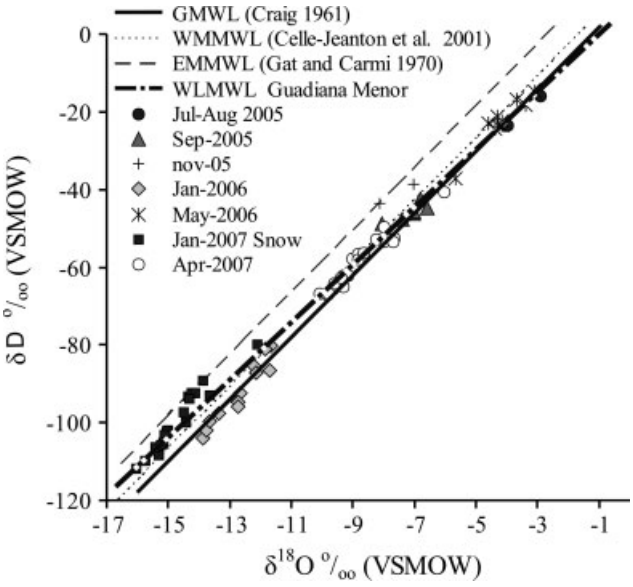

Figure 5. δD versus δ^{18}O plot for the selected more significant precipitation events (individual and monthly)

Seasonal variations. Riesenfeld and Chang (1963a,b) were the first to observe seasonal fluctuations in the isotope contents of precipitation, finding that winter precipitation is lower than that of the summer (Riesenfeld and Chang, 1963a,b; Saxena, 1987). These fluctuations are more marked in places far from the coastal stations, whereas in zones with maritime climates, the seasonal variations are comparatively minor. In temperate climates, where variations in temperature and precipitation follow seasonal trends, there tends to be a parallel variation in the isotope contents.

To detect seasonal effects upon isotope composition we chose station 37, which provided the highest number of samples (Figure 6). The value of δ^{18}O shows a clear seasonal trend (as does D), with higher isotope compositions in warm periods and lower ones in cold periods. This effect is caused by a higher temperature gradient between the source region (ocean) and the precipitation site (continent) during winter, and a lower temperature gradient during summer. No seasonal dependency can be seen as far as *d*-excess is concerned (Figure 6).

Figure 6 reveals a decreasing tendency in the δ^{18}O and δD values over the study period, which is due to a drop in average monthly temperatures in the first months of 2007 compared to the first months of 2006 (www.aemet.es). The seasonal effect is also visible for the entire sampling period at the other sampling locations described in Figure 5.

The graph representing *d*-excess versus precipitation at station 37 clearly shows the influence of rainfall deriving from the Atlantic and the western and eastern Mediterranean, in which fronts arrive from different directions according to no definite pattern.

Continental effect. This effect is one of the factors mentioned in the Introduction that influences the final isotope composition of the precipitation at any one place, and is related to the history of the clouds that generate the precipitation. As they travel over continents cloud masses become depleted in heavy isotopes due to the preferential condensation of this type of molecule. Thus, the precipitation from a single cloud front is more and more negative in δ values the farther it gets from the sea (Clark and Fritz, 1997). This effect is usually observed when using average conditions, although in our study this can also be identified at the level of individual precipitation events, as it is explained in the following paragraph.

Table IV. Values of the parameters from the equation of the LMWL (a) obtained by other researchers in the western (Iberian Peninsula) and central sectors (Italy and Tunisia) of the Mediterranean

Country	Reference	Site	a	b	R^2
Iberian Peninsula		SE Spain All area	7·13	9·75	0·95
		Cazorla (1989–1990)	8·26	23·50	0·94
		Baza (1989–1990)	6·23	4·46	0·93
	Cruz-San Julián *et al.* (1992)	Segura (1989–1990)	8·49	20·06	0·96
		Gador (1989–1990)	7·56	13·37	0·99
		Lújar (1989–1990)	6·56	4·76	0·98
		Doñana (1989–1990)	7·19	5·96	0·97
	Plata (1994)	Península Iber (1962–1988)	7·79 ± 0·62	10·02 ± 2·75	0·95
		Barcelona	7·29	7·29	0·88
	Vandenschrick *et al.* (2002)	Madrid	7·53	5·49	0·96
		Gibraltar	6·19	3·29	0·83
	Andreo *et al.* (2004)	Málaga (1995–1997)	7·00	6·05	0·88
	This research	LMWL Guadiana Menor	7·72	9·99	0·98
		WLMWL Guadiana Menor	7·40	7·24	0·99
Italy		N Italy (1992–2001)	7·71	9·40	0·98
	Longinelli *et al.* (2003)	Central Italy (1992–2001)	7·05	5·61	0·95
		S. Italy (1992–2001)	6·97	7·32	0·95
	Paternoster *et al.* (2008)	S. Italy (2002–2004)	6·56	4·12	0·94
Tunisia		Sfax (1992–1998)	6·70 ± 0·3	3·50 ± 1·3	
	Celle-Jeanton *et al.* (2001)	Tunis (1992–1998)	6·40 ± 0·5	5·20 ± 1·7	
		Tunisia (1968–1998)	5·60 ± 0·2	−(0·80 ± 0·7)	

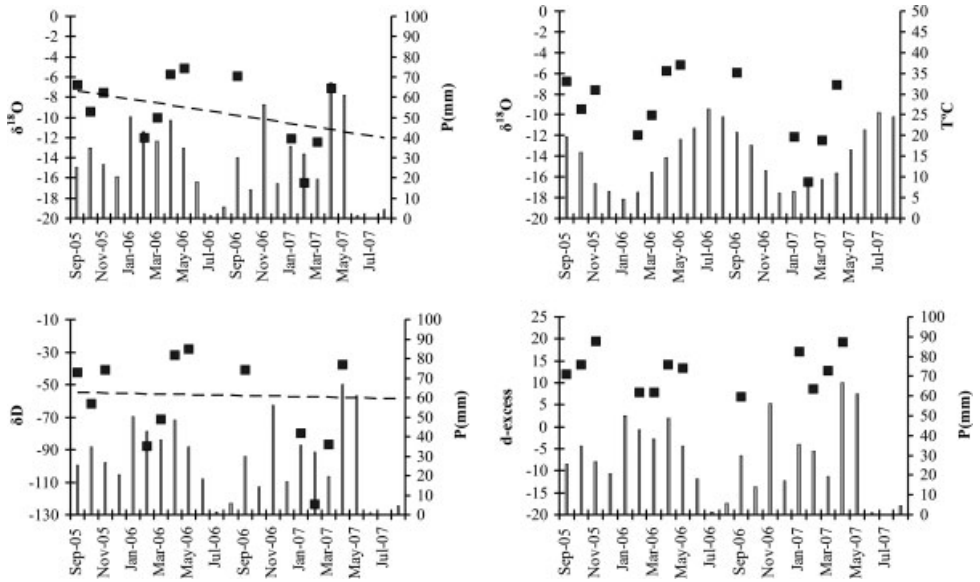

Figure 6. Seasonal variations in $\delta^{18}O$ with precipitation and temperature and in δD and d-excess with precipitation (www.juntadeandalucia.es/. . .) for the station 37 (see Figure 1) from 2005 to 2007. Points represent monthly mean weighted ^{18}O values of rainfall. The columns in the left- and right-hand graphs represent monthly precipitation and average temperature (scales at right)

Despite the complicated orography of the entire area, the presence of fronts originating in both the Atlantic and the Mediterranean and the existence of other modifying effects upon the isotope composition (e.g. the altitude effect), its presence can be detected in rainfall events such as that which took place between 28 and 31 January 2006, produced by a low-pressure cell above the Gulf of Cádiz deriving from the Atlantic (www.inm.es). In the δD versus $\delta^{18}O$ graph, these samples are located along the GMWL (Figure 5). A comparison of stations at similar altitudes reveals a clear trend of decreasing $\delta^{18}O$ values as the distance from the Atlantic Ocean widens in a southwest to northeasterly direction (Figure 7). For example, stations 18, 4 and 34, and 29 and 3 show a decrease in $\delta^{18}O$ of about 1·6–1·9‰ over a distance of some 60 km.

The continental effect is also detectable to a greater extent when studying the monthly rainfall record, such as that carried out in March 2007 (Figure 7), and the mean $\delta^{18}O$ contents from the stations providing most rainfall data. It is in these cases particularly that the rainfall recharge water is enrichment in heavy isotopes in the southeast of the basin and poorer at its northeastern edge, due to the entry of fronts from the Mediterranean. The mixture of precipitation from the Mediterranean (richer in heavy isotopes towards the southeast) and that from the Atlantic (poorer in heavy isotopes as the clouds travel east–northeastwards) recharge the aquifers on the southeast edge of the basin with waters richer in heavy isotopes, compared with the waters along the northeastern edge.

Altitude effect. The decrease in heavy isotopes contained in the precipitation at the higher sampling stations, known as the altitude effect, is caused by the gradual rainout of orographically uplifted air masses. The magnitude of this effect depends upon the morphology of the area and the specific meteorological conditions leading to the formation of precipitation. Published values for the $\delta^{18}O$-altitude relationship vary between −0·15‰ and −0·7‰ per 100 m for $\delta^{18}O$ and −1·2‰ and −5·6‰ per 100 m for δD (Moser and Stichler, 1974; Gat, 1980; Niewodniczanski *et al.*, 1981; Holdsworth *et al.*, 1991). Longinelli and Selmo (2003) reported a gradient of 0·2‰/100 m for Italy. The values of $\delta^{18}O$-altitude gradients compiled by Clark and Fritz (1997) range from 0·2‰/100 to 0·3‰/100.

The altitude curve obtained from one single rainfall event is insufficient to calculate the quantities of groundwater recharge, due mainly to the seasonal effect mentioned elsewhere in this study. This is clearly revealed in the representation of those rainfall events recorded at the highest number of stations (Figure 8). Therefore, because of the variability in precipitation levels in semi-arid climates, sampling for 2 years is not enough to obtain a reliable mean altitude curve. To draw the altitude curves we chose for each rainfall event the stations that present the highest correlation coefficient, sited along a line trending south–southwest to north–northeast (Figure 8).

Despite the complex orography of the basin, the five altitude curves tend to be parallel. The gradient obtained for $\delta^{18}O$ varies within a range of 0·52–0·76‰ per 100 m (Table V), with a mean value of 0·60‰ per 100 m, which is close to the value obtained in the Sierra de Baza after a rainfall event in April 1990, for which the curve was one of 0·57‰ per 100 m (Cruz-San Julián *et al.*, 1992).

Groundwater

To study the isotope content of the groundwater, we chose 20 the most representative points of each aquifer (Table III and Figure 2). The isotope contents of $\delta^{18}O$ and δD in the groundwater were fairly uniform, as it has been pointed out. They vary from −9·90‰ to −6·40‰ and

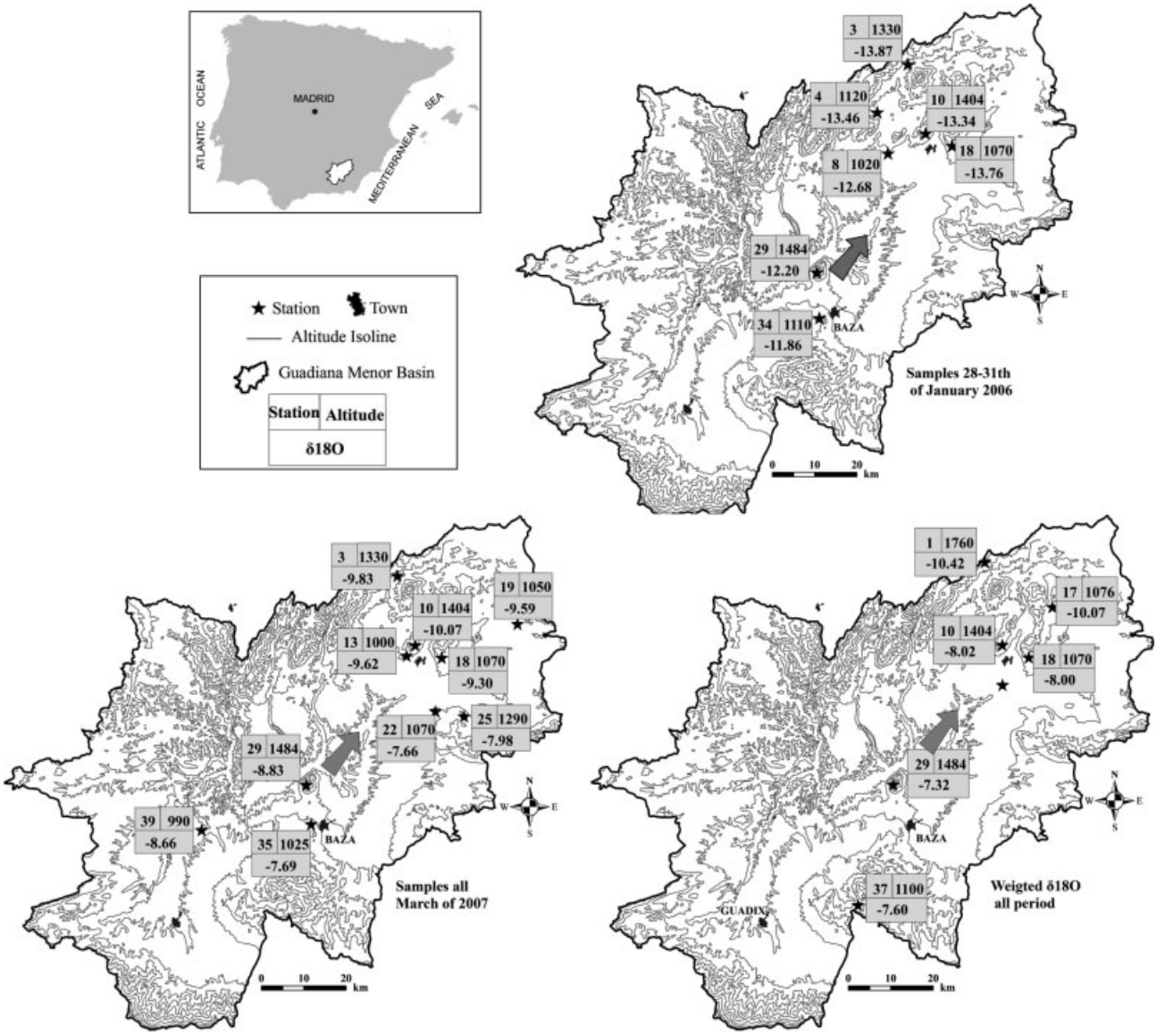

Figure 7. Continental effect indicated by precipitation samples collected in January 2006, April 2007 and all the sampling period at the stations providing the most samples. The arrow indicates the general trend of decrease in the isotope contents

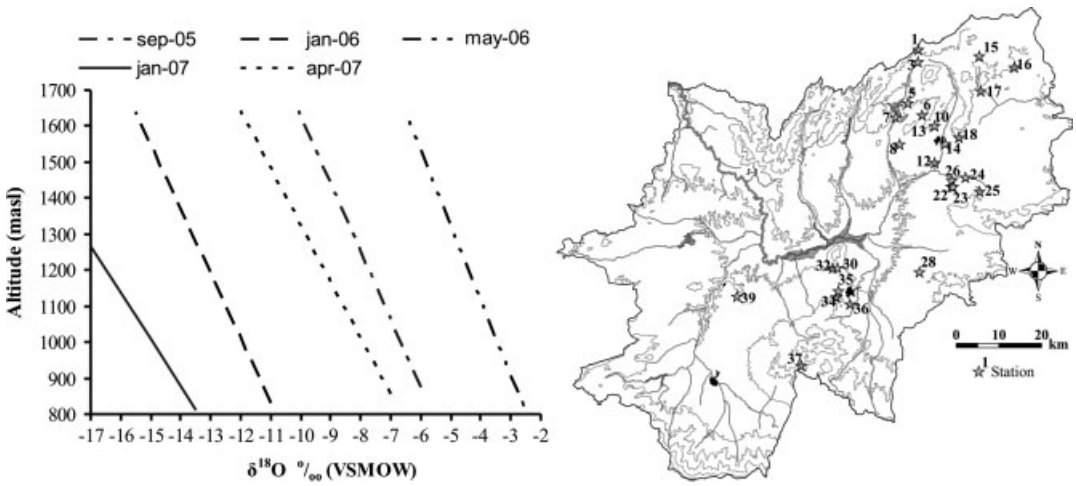

Figure 8. Plot of $\delta^{18}O$ contents versus altitude for precipitation samples collected during different events (individual and monthly sampling). The stations used for the fitting of the altitudinal gradient and the graph of the left (see Table V) are represented in the map (right)

Table V. Equations for the altitude curves of the precipitation events represented by the highest number of samples and altitude gradients obtained

Storm event	Equation	Stations	R^2	Gradient
Sep-05	$y = -190{\cdot}37x - 266{\cdot}66$	1, 6, 10, 12, 17, 18, 37	0·84	0·52‰ per 100 m
Jan-06	$y = -179{\cdot}48x - 1140{\cdot}4$	3, 8, 10, 16, 23, 32, 36	0·77	0·56‰ per 100 m
May-06	$y = -208{\cdot}48x + 288{\cdot}29$	10, 12, 15, 18, 24, 25, 30, 34, 37	0·55	0·52‰ per 100 m
Jan-07	$y = -130{\cdot}6x - 952{\cdot}78$	5, 7, 8, 14, 26, 28, 35	0·89	0·76‰ per 100 m
Apr-07	$y = -157{\cdot}15x - 241{\cdot}75$	3, 5, 10, 15, 22, 24, 30, 35, 39	0·75	0·63‰ per 100 m

−68·69‰ to −48·11‰, with mean values of −8·48‰ to −59·27‰, respectively. The values of *d*-excess range from 12·47‰ to 1·07‰, with a mean of 8·63‰, with lower values found for the well samples (8·23‰) than for the spring samples (9·02‰). Groundwater reflects the weighted mean isotopic precipitation signature in the recharge area. The isotope composition of the groundwater, in which the mean *d*-excess is lower than 10‰, is richer in heavy isotopes than the mean of the precipitation, which reaches a mean value of 12·90‰ (a value that indicates the predominance of rain from the Mediterranean rather than the Atlantic).

The representation of the $\delta D/\delta^{18}O$ values for the isotope composition of the groundwater and shallow water allowed us to obtain the LGWL of the aquifers sampled in the study. The resulting equation is $\delta D = 4{\cdot}79\delta^{18}O - 18{\cdot}64$ ($R^2 = 0{\cdot}86$). The LGWL is characterized by a shallower curve than those obtained for the LMWL and WLMWL, which suggests different evaporation processes from those observed until now, the signature of which is added to the effects of isotope enrichment already seen in the rainfall water.

In Figure 9 the groundwater and shallow-water samples analysed are distinguished by different symbols according to the type of point sampled (well, spring or shallow water) and to the correspondent type of aquifer.

It can be seen in Figure 9 that a series of groundwater and shallow-water points fall between the LMWL and the GMWL, although most of the samples are to the right of the GMWL, suggesting additional evaporation processes.

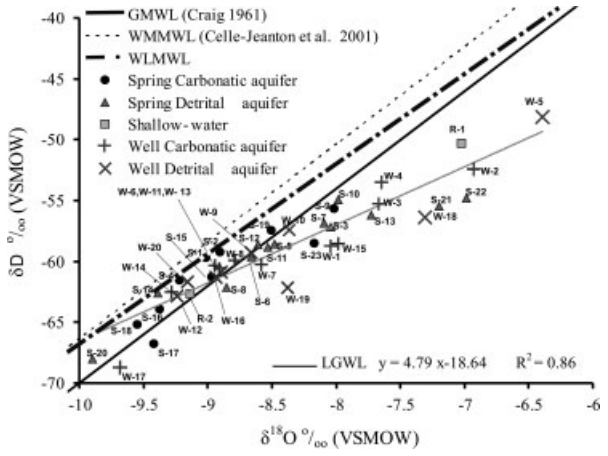

Figure 9. $\delta D/\delta^{18}O$ relationships of groundwater for different aquifers and shallow water. LGWL=local ground water line. For the location of the sampling points see Figure 2

A comparison of the composition of the springs that drain the carbonate aquifer (S-18, S-16, S-4 and S-1, at 1610, 1378, 1510 and 1470 m a.s.l., respectively) reveals that the groundwater become richer in heavy isotopes from the west–southwest towards the east–northeast, a trend which goes against that found in the precipitation waters, which are subject to the continental effect.

If we look at the changes in the isotope content of the springs along a line trending southeast–northwest between points S-13 and S-3 we can see an impoverishment towards the north and northwest, between springs S-13 and S-12, which coincides with the evolution of fronts coming from the Mediterranean and moving north–northwestward, and thus with the continental effect.

According to recent climatic studies carried out in the basin by Fernández-Chacón (2009), during the last 28 years there has been a tendency towards less rainfall arriving from the Atlantic and more from the Mediterranean. This has led to the aquifers in the northeast of the basin, which are more affected by Mediterranean fronts, becoming slightly more enriched in heavy isotopes than those on the north face of the Sierra de Baza and Sierra Nevada, where the Mediterranean influence is less.

The altitude effect on precipitation is also quite evident in the groundwater on comparing springs S-18 and S-17, S-16 and S-15, S-4 and S-6, and well W-8 with S-12, among others, which reveals isotope enrichment from the recharge zones of carbonate aquifers to the centre of the basin and the detrital aquifer discharge zones.

Significant farming activity takes place above the detrital aquifer, particularly in the Llano de Puebla sector to the northeast of the basin, which has resulted in intense exploitation of both the carbonate and detrital aquifers. The wells in these aquifers contain the highest levels of heavy isotopes, with a maximum at W-5, which draws its water from the detrital aquifer (Figures 2 and 2; Table III). This point, together with W-3, W-4 and W-18, are those that show most signs of evaporation effects, which reflects an additional recharge from the return flow of excess irrigation water that has undergone intense evaporation before filtering back into the detrital aquifer.

Another area of considerable farming activity lies to the east–southeast of the town of Baza. The wells we chose to sample have an average depth of some 100 m. The water from these wells, however, shows no signs of evaporation. On the contrary it proved to be more depleted in heavy isotopes, possibly because of

significant groundwater recharge from the Sierra de Baza compared to the quantity of recharge by the infiltration of precipitation.

On the other hand, the sample taken from the San Clemente reservoir (R-1, Figure 9) showed a strong influence of evaporation, typical of lakes and reservoirs with a large expanse of water (Mayr *et al*., 2007; Kohfahl *et al*., 2008b). This reservoir is situated on the carbonate aquifer and so loses water by leakage to the aquifer beneath it. This implies an additional recharge to the latter aquifer and so in wells lower down (e.g. W-2) the water also shows signs of evaporation and enrichment in heavy isotopes.

In the aquifers studied we found subterranean thermal waters and hypothermal waters, reaching temperatures of 26 °C (S-23) and 35 °C (S-19 and W-13) in the carbonate aquifer and between 20 and 41·5 °C in the detrital aquifer (S-20, W-9, S-7, S-8, and S-11). The highest temperatures are associated with points at tectonic accidents between the palaeogeographic domains of the Internal and External zones of the Betic Cordilleras (S-7, S-8, S-12, W-9 and S-23) whilst the coolest thermal springs are associated with tectonic contact zones between subdomains within the Internal and External zones. Thus, when interpreting the isotope content of the groundwater drained or exploited at these points it is important to bear in mind the additional isotope enrichment deriving from the matrix of the aquifer, a process that modifies the $\delta^{18}O$ content with respect to that of δD (Clark and Fritz, 1997).

Until now we have described how the water from the carbonate reliefs around the edges of the basin at higher altitudes are more depleted in isotopes than that of the detrital aquifer situated above the former at lower levels and more towards the centre of the basin (e.g. S-21, S-22 and W-18) (Figures 2 and 9). Nevertheless, at the centre there are also small carbonate outcrops drained and exploited by spring S-19 and well W-13, respectively, samples from which plot between the WLMWL and GMWL (Figure 9). S-19 drains groundwater at 780 m a.s.l. whilst the piezometric level of the water drawn from W-13 is 620 m a.s.l.

According to our observations, it would be normal to expect that at points S-19 and W-13, at the centre of the basin, the water would be significantly affected by evaporation and thus very rich in heavy isotopes, just like the water from spring S-22, which is recharged solely by precipitation and not by farming activity. Nevertheless, the isotope composition at neither of the two former points suggests *a priori* any such evaporation and consequent isotope enrichment effect. This is due to the fact that both carbonate outcrops are fed at depth by hidden water supplies from the Sierra de Baza at higher altitudes and undergo no evaporation processes apart from those affecting the precipitation. When calculating the quantity of recharge in S-19 and W-13 it is necessary to bear in mind that both are fed to some extent by thermal water, the isotope composition of which has been modified by enrichment in $\delta^{18}O$ versus δD in the rock forming the aquifer and also possibly by the mixing of recharge waters within the Sierra de Baza and others filtering into the carbonate aquifer lower down.

CONCLUSIONS

Precipitation reaches the Guadiana Menor basin, mainly in the winter months, from three different sources, which are, of importance: (i) the Atlantic Ocean; (ii) the western Mediterranean Sea and (iii) the eastern Mediterranean Sea.

To characterize the isotope composition of the precipitation waters that recharge the aquifers in the region the WLMWL is more suitable than the LMWL because it takes the quantity of rainfall into account.

The WLMWL and LMWL show a lower curve than the GMWL, WMMWL and EMMWL, above all the WLMWL. This reflects the influence of various modifying effects which bring about enrichment in heavy isotopes. One example of this is the 'amount effect', which takes place mainly from May to September, when increases in the ambient temperature cause rain to evaporate while falling earthwards and/or undergo an exchange with atmospheric vapour. This effect hinders our ability to determine the origin of the weather fronts because it modifies the *d*-excess values.

Apart from the effects of amount and ambient temperature, we also observed seasonal and altitudinal variations in the isotope composition of the rainfall, coinciding with those reported in the literature. The altitude gradients obtained for $\delta^{18}O$ are high, ranging between 0·52‰ and 0·76‰.

The final effect on the precipitation in this basin that we have identified is the continental effect. The mixture of fronts deriving both from the Atlantic and the Mediterranean determines the existence of a zone in the southeast where the waters are quite rich in heavy isotopes, a zone in the north–northeast where the waters are relatively depleted of these isotopes and an intermediate zone in the west-central part of the basin on the northern flank of the Sierra de Baza.

The groundwater, for their part, is in general richer in heavy isotopes than the precipitation water, particularly on the slopes of the mountains and at lower levels towards the centre of the basin. This can be put down to the fact that most of the groundwater has undergone additional evaporation processes, including evaporation in the aquifer itself (more so in the detrital aquifers than in the carbonate ones), recharge from irrigation return flows, the water from which presents strong signs of evaporation and/or effects caused by additional recharge from water deriving from reservoirs.

Through the isotope composition of the groundwater and precipitation we have been able to detect the existence of hidden subterranean recharge from the carbonate aquifers, mainly from the Sierra de Baza, into the neighbouring detrital aquifers or even into other carbonate aquifers in the centre of the basin.

ACKNOWLEDGEMENTS

This research was funded by the Geological Survey of Spain, IGME, and carried out under the auspices of an agreement between IGME, Granada University, the Freie Universität Berlin and the Alfred Wegener Institute (Potsdam). We thank Mr Ricardo (Gor) for his support during field work. We also thank A. L. Tate for translating and correcting our text. We acknowledge the comments of two anonymous reviewers which have improved the last version of this article.

REFERENCES

Andreo B, Liñán C, Jiménez-Cisneros C, Caballero F, Mudry J. 2004. Influence of rainfall quantity on the isotopic composition (^{18}O and ^{2}H) of water in mountainous areas. Application for groundwater research in the Yunquera-Nieves karst aquifers (S Spain). *Applied Geochemistry* **19**: 561–574.

Aouad A, Travi Y, Blavoux B, Job J-O, Najem W. 2004. Isotope study of snow and rain on Mount Lebanon: preliminary results. *Hydrological Sciences Journal* **49**(3): 429–441.

Bowen GJ, Revenaugh J. 2003. Interpolating the isotopic composition of modern meteoric precipitation. *Water Resources Research* **39**(10): Art no.1299.

Celle-Jeanton H, Travi Y, Zouari K, Daoud A. 2001. Caractérisation isotopique des pluies en Tunisie. Essai de Typologye dans la région de Sfas. *Comptes-rendus de l'Académie des Sciences* **333**: 625–631.

Clark I, Fritz P. 1997. *Environmental Isotopes in Hydrogeology*. Lewis Publishers: NY.

Craig H. 1961a. Isotopic variations in meteoric waters. *Science* **133**: 1702–1703.

Craig H. 1961b. Standards for reporting concentrations of deuterium and oxygen-18 in natural waters. *Science* **133**: 1833–1834.

Cruz-San Julián JJ, Araguas L, Rozanski K, Benavente J, Cardenal J, Hidalgo MC, García López S, Martínez Garrido JC, Moral F, Olias M. 1992. Sources of precipitation over South-Eastern Spain and groundwater recharge. An isotopic study. *Tellus* **44B**: 226–236.

Dansgaard W. 1953. The abundance of 18O in atmospheric water and water vapour. *Tellus* **5**(16): 461–469.

Dansgaard W. 1961. The isotopic composition of natural water. *Meddelelser* ***om Gronland*** **165**(2): 120 pp.

Delgado A, Núñez R, Caballero E, Jiménez de Cisneros C, Reyes E. 1991. Composición isotópica del agua de lluvia de Granada. *IV. Congreso Geoquímica de España*. Monografía, 350–358.

Ehhalt D, Knott K, Nagel JF, Vogel JC. 1963. Deuterium and oxygen-18 in rain water. *Journal of Geophysical Research* **68**: 3775–3780.

Fernández-Chacón F. 2009. *Contribución al conocimiento hidrogeológico de una depresión interna en clima mediterráneo semiárido (Cabecera del Guadiana Menor, Cordillera Bética)*. Tesis Doctoral, 387 pp.

Friedman I, Machta L, Soller R. 1962. Water vapour exchange bteween a droplet and its environment. *Journal of Geophysical. Research* **67**: 2761–2766.

Frot E, Van Wesemael B, Vandenschrick G, Souchez R, Sole-Benet A. 2007. Origin and type of rainfall for recharge of a karstic aquifer in the western Mediterranean: a case study from the Sierra de Gador-Campo de Dalias (Southeast Spain). *Hydrological Processes* **21**: 359–368.

Gat JR, Carmi I. 1970. Evolution of the isotopic composition of the atmospheric water in the Mediterranean Sea area. *Journal of Geophysical Research* **75**: 3039–3048.

Gat JR, Carmi I. 1987. Effect of climate changes on the precipitation patterns and isotopic composition of water in a climate transition zone: case of the Eastern Mediterranean Sea area. In: *The Influence of Climate Change and Climatic Variability on the Hydrologic Regime and Water Resources*. Proc. Vancouver Symp., August. IAHS Pub. no. 168. 513–523.

Gat JR. 1980. The isotopes of hydrogen and oxygen in precipitation. In: Fritz P, Fontes J-Ch (Eds). *Handbook of Environmental Isotope Geochemistry, vol. 1*. Elsevier: Amsterdam; 21–47.

Gat JR, Dansgaard W. 1972. Stable isotope survey of fresh water occurrences in Israel and the Jordan Rift Valley. *Journal of Hydrology* **16**: 177–211.

Gat JR, Matsui E. 1991. Atmospheric water balance in the Amazon basin: An isotopic evapotranspiration model. *Journal Geophysical Research* **96**: 13179–13188.

Gedzelman SD, Lawrence JR, White JWC, Smiley D. 1987. The isotopic composition of precipitation at Mohok lake, New York: The amount effect. *Journal Geophysical Research* **92**(D1): 1033–1040.

Gonfiantini R. 1978. Standards for stable isotope measurements in natural compounds. *Nature* **271**: 534–536.

Holdsworth G, Fogarasi S, Krouse H. 1991. Variation of the stable isotopes of water with altitude in the Saint Elias Mountains of Canada. *Journal of Geophysical Research* **96**(D4): 7483–7494.

IAEA. 2001. *GNIP Maps and Animations*, International Atomic Energy Agency: Vienna. Available from (http://isohis.iaea.org/).

Jouzel J, Merlivat L. 1984. Deuterium and oxygen 18 in precipitation: modelling of the isotopic effect during snow formation. *Journal of Geophysical Research* **89**: 11748–11757.

Kohfahl C, Sprenger Ch, Benavente J, Meyer H, Fernández-Chacón F, Pekdeger A. 2008a. Characterisation of groundwater recharge in a semiarid karstic environment by means of stable isotopes and hydrogeochemical data. *Applied Geochemistry* **23**: 846–862.

Kohfahl C, Rodríguez M, Fenk C, Menz Ch, Benavente J, Hubberten H, Meyer H, Paul L, Knappe A, López-Geta JA, Pekdeger A. 2008b. Characterising flow regime and interrelation between surface-water and ground-water in the Fuente de Piedra salt lake basin by means of stable isotopes, hydrogeochemical and hydraulic data. *Journal of Hydrology* **351**: 170–187.

Longinelli A, Selmo E. 2003. Isotopic composition of precipitation in Italy: a first overall map. *Journal of Hydrology* **270**: 75–88.

Mayr Ch, Lücke A, Stichler W, Trimborn P, Ercolano B, Oliva G, Ohlendorf Ch, Soto J, Fey M, Haberzettl T, Jansen S, Schäbitz F, Scheleser G, Wille M, Zolitschka B. 2007. Precipitation origin and evaporation of lakes in semi-arid Patagonia (Argentina) inferred from stable isotopes (δ^{18}O, δ^{2}H). *Journal of Hydrology* **334**: 53–63.

Meyer H, Schönicke L, Wand U, Hubberten H-W, Fridrichsen H. 2000. Isotope studies of hydrogen and oxygen in Ground Ice. Experiences with the equilibration technique. *Isotopes in Environmental and Health Studies* **36P**: 133–149.

Moser H, Stichler W. 1974. Deuterium and oxygen-18 contents as an index of the properties of snow covers. In *Symposium on snow mechanisms*. IAHS Publications no. **114**: 122–135.

Niewodniczanski J, Grabczak J, Baranski W, Rzepka J. 1981. The altitude effect on the isotopic composition of snow in high mountains. *Journal of Glaciology* **27**: 99–111.

OIEA. 1996. *Programa OIEA/OMM sobre la composición isotópica de la precipitación: Global Network of Isotopes in Precipitation (GNIP)*. Vienna, September 1996.

Paternoster M, Liotta M, Favara R. 2008. Stable isotope ratios in meteoric recharge and groundwater at Mt. Vulture volcano, southern Italy. *Journal of Hydrology* **348**: 87–97.

Plata A. 1994. *Composición isotópica de las precipitaciones de la Península Ibérica*. *Centro de Estudios y Experimentación de Obras Públicas*, vol 39. Madrid: Spain.

Riesenfeld EH, Chang TL. 1963a. Uber den Gehalt an HDO und H218O in Reben un Schnee. *Berichte der Durstigen Chemischen Gesellschaft Jahrgang* **69**: 1305–1307.

Riesenfeld EH, Chang TL. 1963b. Uber die Vertilung der schweren Waserisotopen auf der Erde. *Berichte der Durstigen Chemischen Gesellschaft Jahrgang* **69**: 1308–1310.

Rindsberger M, Magaritz M, Carmi I, Gilad D. 1983. The relation between air mass trajectories and the water isotope composition in the Mediterranean Sea area. *Geophysics Review Letters* **10**: 43–46.

Saxena RK. 1987. *Oxygen-18 fractionation in nature and estimation of groundwater recharge* (Report). Uppsala University, Department of Physical Geography. Division of Hydrology.

Vandenschrick G, Van Wesemael B, Frot E, Pulido-Bosch A, Molina L, Stievenenard M, Souchez R. 2002. Using stable isotope analysis to characterize the regional hydrology of the Sierra de Gador, S-E Spain. *Journal of Hydrology* **265**: 43–55.

http://www.aemet.es.

http://www.inm.es/es/eltiempo/observacion/satelite/masas.

http://www.juntadeandalucia.es/medioambiente.

